IEEE Photonics Journal
An IEEE Photonics Society Publication

Open Access

Dual-Comb Absolute Distance Measurement Based on a Dual-Wavelength Passively Mode-Locked Laser

Volume 9, Number 6, December 2017

Baike Lin
Xin Zhao
Mingzhao He
Yingling Pan
Jie Chen
Shiying Cao
Yige Lin
Qiang Wang
Zheng Zheng
Zhanjun Fang

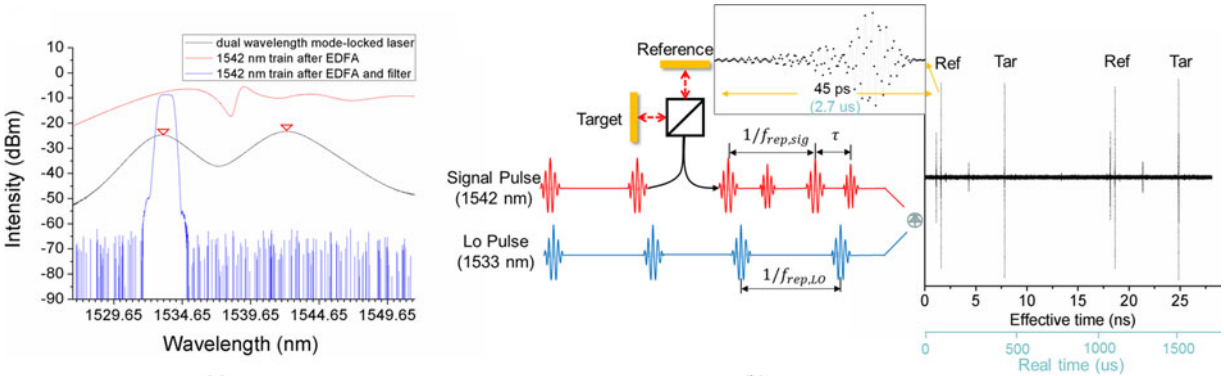

DOI: 10.1109/JPHOT.2017.2772292
1943-0655

Dual-Comb Absolute Distance Measurement Based on a Dual-Wavelength Passively Mode-Locked Laser

Baike Lin,[1,2] Xin Zhao,[3] Mingzhao He,[1] Yingling Pan,[3] Jie Chen,[3] Shiying Cao,[1] Yige Lin,[1] Qiang Wang,[1] Zheng Zheng,[3,4] and Zhanjun Fang[1,2]

[1]National Institute of Metrology, Beijing 100029, China
[2]The Institute of Instrument Science and Technology, Department of Precision Instrument, Tsinghua University, Beijing 100084, China
[3]School of Electronic and Information Engineering, Beihang University, Beijing 100083, China
[4]Collaborative Innovation Center of Geospatial Technology, Wuhan 430079, China

DOI:10.1109/JPHOT.2017.2772292

Manuscript received September 15, 2017; revised November 3, 2017; accepted November 7, 2017. Date of publication November 10, 2017; date of current version November 22, 2017. This work was supported in part by the National Natural Science Foundation of China (NSFC, 91336212, 91436104, 61435002, 61521091, 61675014, and 61675015) and in part by the National Key R&D Program of China (2016YFF0200201 and 2016YFF0200405). Corresponding author: Baike Lin (e-mail: linbk@nim.ac.cn).

Abstract: A new absolute distance measurement system is demonstrated in this paper, which is based on a dual-wavelength passive mode-locked fiber laser. By controlling the intracavity loss and spectral filtering, the cavity mode-locked by a single-wall carbon nanotube saturable absorber is able to generate two pulse trains at slightly different repetition rates simultaneously with high mutual coherence. Comparisons with the commercial interferometers located on the 80-m large-scale dimensional standard show a combined measurement uncertainty of $6\,\mu\,m + 1 \times 10^{-7} L$ ($k = 2$), in an averaging time of 1 s. Our compact dual-comb system provides a low-cost way for ranging, with continuous range, rapid measurement, and high resolution.

Index Terms: Erbium lasers, heterodyning, mode-locked lasers, carbon nanotubes and confined systems.

1. Introduction

The primary motivation for the development of the optical frequency comb (OFC) was to bridge the optical clocks between other radio frequency standards or clocks [1], that is, a frequency ruler from optical frequency to radio frequency with fractional uncertainties of 10^{-19} or lower [2]. However, the utility of the frequency comb has been expanded well beyond optical frequency metrology [3], and it could be used in many other areas, such as time/frequency transfer [4], arbitrary optical waveform generation [5], and molecular spectroscopy [6]. Moreover, as a frequency comb is composed of an ideal regular train of pulses in time domain and equally spaced spectral lines in frequency domain, ranging methods using frequency combs based on either time-of-flight (TOF)

measurement of the elapsed time between the optical pulses or measuring the optical interference fringes could realize a large ambiguity range and high precision simultaneously [7]. Particularly, precise large-scale dimensional metrology up to hundreds of meters or larger is necessary in high-end equipment manufacturing, aerospace engineering, and other frontier sciences. Since the first experiment by Minoshima in 2000 [8], great efforts had been made to this area with various proposed approaches [9]–[13]. While these works used only one comb, there is another way of using two combs simultaneously with slightly different repetition rates. During the measuring procedure, one of the comb used as the local oscillator (LO), samples the pulses of the other comb (signal) temporally, to obtain the asynchronous optical sampling signals from which the distance is calculated. Compared to the traditional TOF measurements, one of the advantages of this approach is the greatly relaxed requirement on the bandwidth of the photodetector, by down-converting the ultrafast optical pulse to a time-stretched version of much lower bandwidth. The ability to make rapid measurement is another advantage, particularly in the applications that need real-time feedback. Finally, absolute distance measurement can be realized without mechanical delay scanning devices like lead rails, in contrast to those traditional laser interferometers applicable to displacement measurements only. The dual-comb system was firstly demonstrated by I. Coddington from NIST (National Institute of Standards and Technology, USA) in 2009 [14]. By calculating the pulse TOF and the optical carrier phase, the precision reached 5 nm at 60 ms. However, the system was costly as the two uncorrelated frequency combs need to be phase-locked to an ultra-stable cavity respectively in order to synchronize the pulse trains of the two combs and reach high interferometric precision. More recently, alternative schemes to generate asynchronous dual-comb with high passive mutual coherence has become an attractive research trend. Several different approaches were explored in the past few years: two asynchronous trains of pulses emitted from the same mode-locked laser cavity [15], [16], two cavities pumped by the same pump laser [17], [18], and two sets of electro-optic modulated combs seeded by the same cw laser [19], [20]. While some of them had been applied to molecular spectroscopy, these dual-comb sources could also be used for ranging measurements. In all these schemes the first one shows the highest mutual coherence between the two combs compared to the others as the two asynchronous pulse trains come from the same optical cavity, thus should provide the potential for the highest precision.

In this letter, we propose and develop an absolute distance measurement system using a dual-wavelength passive mode-locked fiber laser [21]. The laser is able to generate two pulse trains at different center wavelengths simultaneously, by using a single-wall carbon nanotube (SWNT) as a saturable absorber. After optical filtering and amplifying, these two independent pulse trains could be used to configure a dual-comb system for absolute distance measurement. The system is compared with the 80-Meter Large-Scale Dimensional Standard at NIM (National Institute of Metrology, China), showing a compact and low-cost way for absolute distance measurement with continuous range and high resolution.

2. Principle

The principle of our absolute distance measurement scheme is shown in Fig. 1. The pulse train denoted as the signal pulse train (marked in red) is transmitted into a Michelson Interferometer (MI) and split into two pulse trains: the reference pulse train and the target pulse train, reflected from the reference mirror and the target mirror respectively. These two pulse trains are respectively overlapped with the local pulse train (marked in blue) and then detected by a balanced photodetector whose output is digitized, yielding the interferograms on the right, which could be used to calculate the value of the distance. Mathematically, expressions of the two signal pulse trains and the local pulse trains could be described as below:

$$E_{\text{ref}} = \sum_{m} A_m \cos[2\pi(m f_{\text{rep,sig}} + f_{\text{ceo,sig}})t] \tag{1}$$

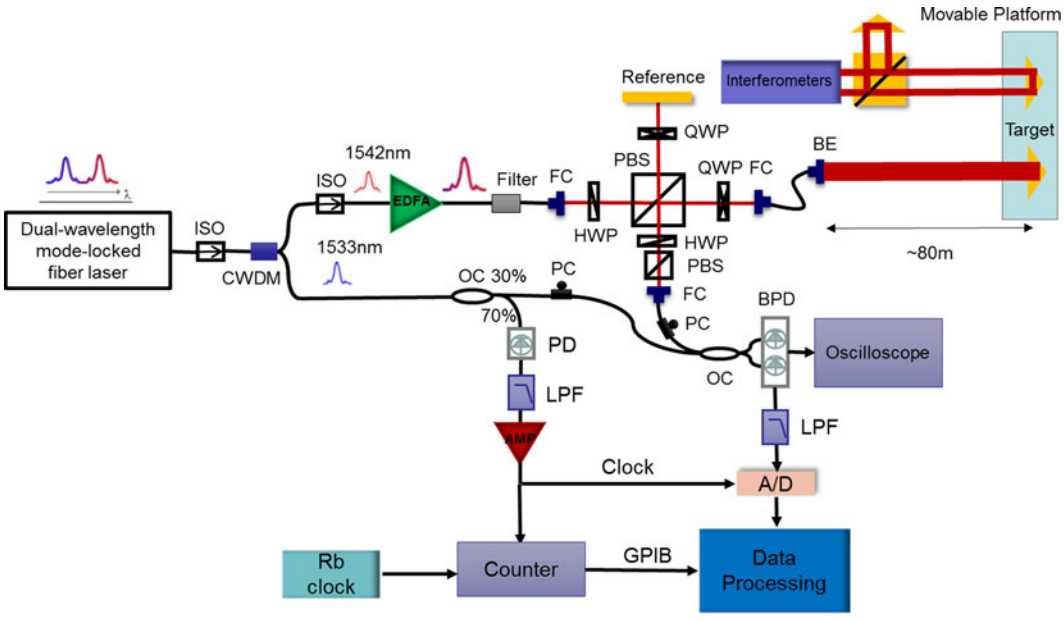

Fig. 1. Principle of the dual-comb absolute distance measurement system using the temporal asynchronous optical sampling technique. The cross-correlation interferograms digitized in the real time scale (lower scale) and the effective time scale (upper scale) are shown on the right. The reference pulse and the target pulse are labeled, while the others are spurious reflections.

$$E_{\text{tar}} = \sum_m A_m \cos[2\pi(mf_{\text{rep,sig}} + f_{\text{ceo,sig}})(t-\tau)] \tag{2}$$

$$E_{LO} = \sum_n B_n \cos[2\pi(nf_{\text{rep},LO} + f_{\text{ceo},LO})t] \tag{3}$$

where E_{ref} and E_{tar} are the electrical fields of the signal pulses reflected from the reference arm and the target arm, $f_{\text{rep,sig}}$ and $f_{\text{ceo,sig}}$ are their repetition rates and the carrier-envelope offset frequencies. $\tau = 2Ln_g/c$ is the delay time between the reference arm and the target arm, where n_g is the group refractive index at the carrier frequency. E_{LO} represents the LO pulse, whose repetition rate and carrier-envelope offset rate are $f_{\text{rep},LO}$ and $f_{\text{ceo},LO}$. According to the theory of the optical interference, the interferograms expressions could be described as $|E_{\text{ref}} + E_{LO}|^2$ and $|E_{\text{tar}} + E_{LO}|^2$. The DC terms are eliminated when the balanced photodetector is used, only the correlative term $2E_{\text{ref}}E_{LO}$ or $2E_{\text{tar}}E_{LO}$ is reserved, which could be expressed as below:

$$I_{\text{ref}}(i\Delta f_{\text{rep}}) = 2\sum_i A_m B_n \cos[2\pi(i\Delta f_{\text{rep}} + f_{\text{ceo},LO} - f_{\text{ceo,sig}})t] \tag{4}$$

$$I_{\text{tar}}(i\Delta f_{\text{rep}}) = 2\sum_i A_m B_n \cos[2\pi(i\Delta f_{\text{rep}} + f_{\text{ceo},LO} - f_{\text{ceo,sig}})t + 2\pi(mf_{\text{rep,sig}} + f_{\text{ceo,sig}})\tau] \tag{5}$$

Here Δf_{rep} is the repetition rate difference between $f_{\text{ref,sig}}$ and $f_{\text{rep},LO}$. And i represents the mode number of the down-converted radiofrequency spectrum. Thus, the phase difference between the reference and target interference signals at the corresponding frequencies could be expressed as below:

$$\varphi(i\Delta f_{\text{rep}}) = 2\pi(mf_{\text{rep,sig}} + f_{\text{ceo,sig}})\tau \tag{6}$$

A simple linear fit of the equation gives the slope $b = \Delta\varphi(\Delta f_{\text{rep}})/f_{\text{rep,sig}} = 4\pi Ln_g/c$, so the distance L can be expressed as:

$$L = \frac{\Delta\varphi(\Delta f_{\text{rep}})c}{4\pi f_{\text{rep,sig}} n_g} \tag{7}$$

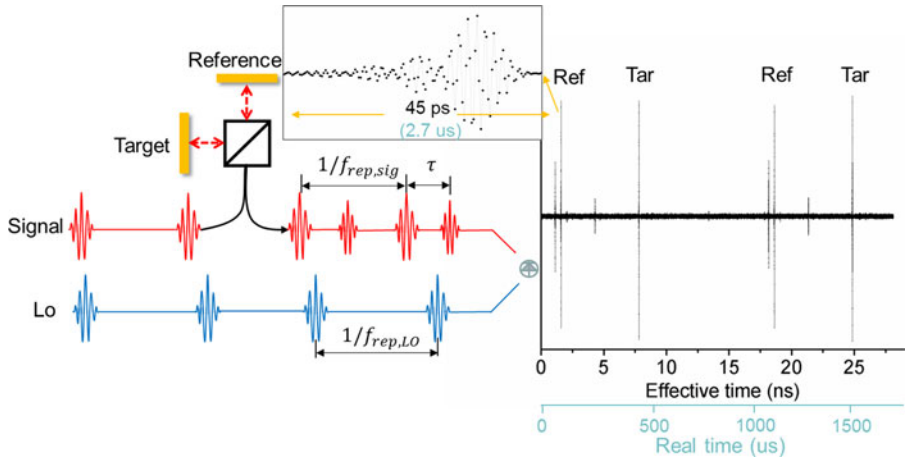

Fig. 2. Experimental setup of the dual-comb absolute distance measurement system based on a dual-wavelength mode-locked fiber laser. ISO: optical isolator, CWDM: coarse wavelength division multiplexer, EDFA: Er-doped fiber amplifier, OC: optical coupler, PC: polarization controller, FC: fiber collimator, BE: beam expander, PBS: polarization beam splitter, HWP: half wave plate, QWP: quarter wave plate, LPF: lowpass filter, AMP: amplifier, A/D: analog-to-digital converter, PD: photodetector, BPD: balanced photodetector.

Here c is the vacuum velocity of light, and the group refractive index n_g is calculated at the measured atmospheric conditions [22], including the temperature, the atmospheric pressure, the percentage of humidity and the level of carbon dioxide. As the item $\Delta\varphi(\Delta f_{\text{rep}})$ has a range of $(0, 2\pi)$, the unambiguity range of the measurement is $c/2f_{\text{rep,sig}}n_g$, approximately several meters when the repetition rate is dozens of MHz. When the distance to be measured is larger than the unambiguity range, the expression could be written as below:

$$L = \left(\frac{\Delta\varphi(\Delta f_{\text{rep}})}{2\pi} + N\right) \cdot \frac{c}{2f_{\text{rep,sig}}n_g} \tag{8}$$

The integer N could be obtained from a priori knowledge, or be measured by some simple schemes as the unambiguity range is quite large. In our experiment, the nominal distance is given by three commercial interferometers used in the ranging system.

3. Experimental Setup

The schematic diagram of our system is shown in Fig. 2, which is based on a dual-wavelength mode-locked Er-doped fiber laser, is supported by Beihang University. By carefully adjusting an optical fiber polarization controller (PC) inside the cavity of the laser, we could obtain two mode-locked pulse trains simultaneously. The two peaks, centered at 1533 nm and 1542 nm wavelength, represent two different pulse trains respectively. The repetition rates of the two pulse trains are around 58.691 MHz, with a slight difference of ~1 kHz. Here we designate the 1533 nm pulse train as the local oscillator (LO), while the 1542 nm pulse train as the signal pulse train. After passing through an optical fiber isolator (ISO), the two pulse trains are split into two arms by a Coarse Wavelength Division Multiplexer (CWDM) fiber. Then the 1533 nm pulse train is divided into two parts. The majority, about 70%, is detected by an InGaAs photodetector (ET-3000A, EOT). After electrical filtering and amplifying, the repetition rate of the 1533 nm pulse train is acquired, with the signal-to-noise ratio (SNR) of more than 40 dB. The rf signal is used to not only clock the digitizer but also give the repetition rate for calculating the distance. The rest portion of the 1533 nm pulse train, after traveling through an optical fiber polarization controller (PC), is used for sampling the 1542 nm pulse train (the signal pulse). In the signal arm, there is an Er-doped fiber amplifier (EDFA), which amplifies and spectrally broadens the 3 dB bandwidth of the signal pulse from the initial 3 nm to 60 nm through fiber nonlinearities. Therefore, the LO and signal pulses can spectrally overlap

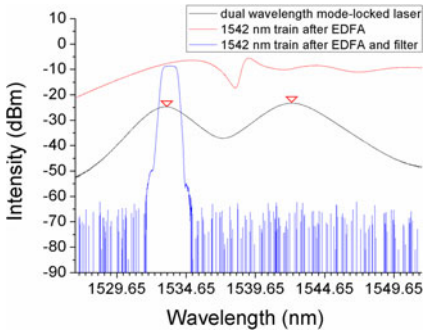

Fig. 3. The optical spectrum of the output of the dual-wavelength mode-locked laser, the 1542 nm train after EDFA, and the 1542 nm train after EDFA and filter.

around 1533 nm. A ∼1.5 nm bandpass filter (i.e., a 200 GHz DWDM filter) limits the transmitted optical bandwidth in order to meet the Nyquist condition for sampling. The optical spectrum of the output of the dual-wavelength mode-locked laser, the 1542 nm train after EDFA, and the 1542 nm train after EDFA and filter, are shown in Fig. 3.

After filtering, the signal pulse is split into the reference arm and the target arm of a Michelson Interferometer (MI) by a polarization beam splitter (PBS). The retro-reflector in the reference arm is fixed, while the one in the target arm is movable as it is mounted on an 80-meter high-accuracy guide rail. The beam of the target arm is coupled back into a ∼2 m piece of single mode fiber through a fiber collimator (FC) after the PBS, before the light finally launched by an optical beam expander (BE10M-C, Thorlabs) towards the target retro-reflector mounted on a movable platform of the guide rail. The reflected beams from both the target and reference are recombined after the PBS, by using the quarter wave plate (QWP) and coupled into fiber through another FC. The LO pulse and the signal pulses enter a 2 × 2 fiber coupler, whose outputs are connected to a balanced photodetector (PDB420C, Thorlabs). The time-domain interferograms are digitized by an A/D converter (PCI-5122, National Instruments) for data processing. The A/D converter is clocked by the repetition rate of the LO pulse train. The distance measurement results are compared with three commercial interferometers (5519B, Agilent) located on the same end of the rail, which monitor the motion of the platform.

4. Results

The process of retrieving the phase difference $\Delta\varphi(i\,\Delta f_{\text{rep}})$ from the FFT phase spectrum to determine the absolute distance is shown in Fig. 4. According to (7), The measured distance is calculated from the phase difference $\Delta\varphi(\Delta f_{\text{rep}})$ between the unwrapped reference and target FFT phase spectrum, which are derived from their respective interferograms, shown in Fig. 4(d). The calculated reference phase spectrum and its unwrapped spectrum are shown in Fig. 4(b) and (c). The calculating range is limited from 10700 to 11200 in order to obtain the highest signal-to-noise ratio, according to the amplitude spectrum shown in Fig. 4(a).

The performance of our system is tested by comparing the results with the interferometers located on the 80-Meter Large-Scale Dimensional Standard. The stability of the system is evaluated by the Allan deviation over different averaging times at a fixed position. Fig. 5(a) shows the Allan deviation of the results at the position of 70 m. It is clear that the Allan deviation is about 181 μm for 1 ms, and reduced to 2.8 μm for 1 s. Fig. 5(b) shows the ranging results when compared with those interferometers at eight different positions, from 1 m to 70 m. The absolute values of the residuals and their standard deviations are all within 10 m, for an averaging time of 1 s. According to (7), the uncertainty of the measurement is related to the air refractive index n_g, the repetition rate of the signal pulse $f_{\text{rep,sig}}$, and the phase difference $\Delta\varphi(\Delta f_{\text{rep}})$. So the relative uncertainty of L can be

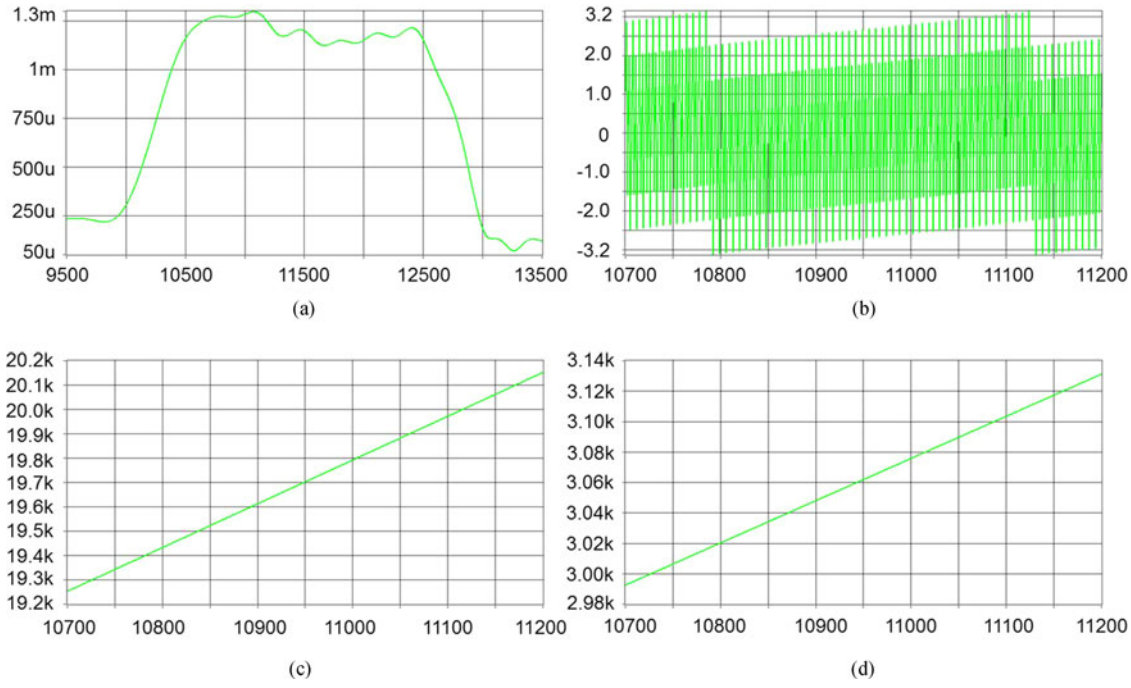

Fig. 4. The process of retrieving $\Delta\varphi(i\Delta f_{rep})$ from the FFT phase spectrum to determine the absolute distance. (a) The FFT amplitude spectrum of the reference interferograms. (b) The FFT phase spectrum of the reference interferograms. (c) The unwrapped FFT phase spectrum of the reference interferograms. (d) The phase difference between the unwrapped reference and target FFT phase spectrum.

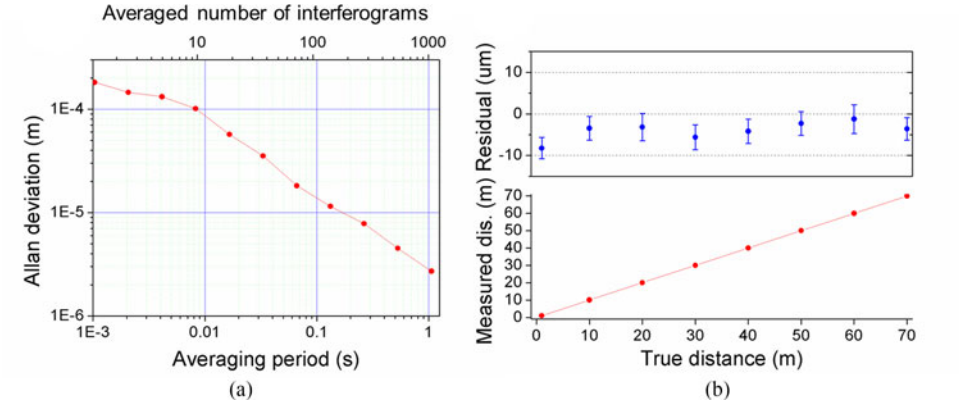

Fig. 5. The performance of the absolute distance measurement system comparing with interferometers. (a) Allan deviation of the comparisons at the distance of 70 m. (b) The residuals and their standard deviations of the ranging results at different distances, from 1 m to 70 m.

expressed as below:

$$\frac{\delta L}{L} = \sqrt{\left(\frac{\delta n_g}{n_g}\right)^2 + \left(\frac{\delta f_{rep,sig}}{f_{rep,sig}}\right)^2 + \left(\frac{\delta \Delta\varphi}{\Delta\varphi}\right)^2} \tag{9}$$

The uncertainty of the air refractive index n_g has an inherent uncertainty of Ciddor formula 2×10^{-8}, and the inaccuracy of the measured atmospheric conditions. We have estimated the laboratory environmental factors, such as air temperature, pressure and humidity, and concluded that the measurement uncertainty of air refractive index is better than 1×10^{-7}. The uncertainty of the repetition rate of the signal pulse is estimated to be much lower than 1×10^{-8} during the

measurement time by monitoring the repetition rate of the LO pulse and calculating the repetition rate difference, so the contribution of the second term of the (9) can be neglected. The third term comes from the uncertainty of the delay time between the reference and the target signals in the effective time scale. We give this value to be 20 fs simply from an estimation of the standard deviation of the delay time in the effective time scale after an averaging time of 1 s, which is 6 μm for distance. The evaluation is validated as it is consistent with the stability of the system shown in Fig. 5(a), while the other impacts like the air refractive index and the repetition rate are steady in a short averaging time. Therefore, the combined uncertainty is estimated to be 6 μm when the distance is less than the unambiguity range, and $6\mu\ m + 1 \times 10^{-7} L$ ($k = 2$) for longer range, such as 70 meters distance, by considering the influence of the air refractive index n_g, which shows good agreement with the data of the results in Fig. 5(b). For instance, the uncertainty is 13 μm at the distance of 70 m, or a relative uncertainty of 1.9×10^{-7}.

5. Conclusion

In summary, we demonstrate a dual-comb absolute distance measurement system using the method of temporal asynchronous optical sampling, enabled by a dual-wavelength mode-locked fiber laser instead of two mode-locked lasers. By generating two pulse trains with slightly different repetition rates in one optical cavity simultaneously, a high mutual coherence of these two pulse trains is observed. Through Fourier analysis of the spectral phase information of the interferogram, the delay time between the target pulse and the reference pulse can be calculated, so is the distance. The measurement results are compared with those from interferometers located on the 80-Meter Large-Scale Dimensional Standard at NIM with an uncertainty of $0.1\ \mu\ m + 1 \times 10^{-7} L$ ($k = 2$). The results show that the residuals and their standard deviations are all within 10 μm after an averaging time of 1 s. The measurement uncertainty is estimated to be $6\ \mu\ m + 1 \times 10^{-7} L$ ($k = 2$), according to the comparisons above and the uncertainty of the air refractive index. Besides the air refractive index, the uncertainty is dominated by the spreading of the delay time between the target pulse and the reference pulse, which could be resulted from the laser. A lower noise source could be chosen for pumping, so does a better design of the cavity to reduce the influences of temperature, the sound and air flow. Optimization of the repetition rates and their difference could also lead to a better precision as suggested by previous theoretical studies [23]. Besides, a loose electrical locking of the repetition rate to an rf reference like a Rubidium clock may help to remove the repetition rate drift, and thus improves the stability of the system.

Acknowledgment

The authors thank H. Shi from Tianjin University for help of calculating the group refractive index.

References

[1] T. Udem, R. Holzwarth, and T. W. Hnsch, "Optical frequency metrology," *Nature*, vol. 416, no. 6877, pp. 233–237, 2002.
[2] L. Ma *et al.*, "Optical frequency synthesis and comparison with uncertainty at the 10^{-19} level," *Science*, vol. 303, no. 5665, pp. 1843–1845, 2004.
[3] N. R. Newbury, "Searching for applications with a fine-tooth comb," *Nat. Photon.*, vol. 5, no. 4, pp. 186–188, 2011.
[4] J. Kim, J. A. Cox, J. Chen, and F. X. Krtner, "Drift-free femtosecond timing synchronization of remote optical and microwave sources," *Nat. Photon.*, vol. 2, no. 12, pp. 733–736, 2008.
[5] S. T. Cundiff and A. M. Weiner, "Optical arbitrary waveform generation," *Nat. Photon.*, vol. 4, no. 11, pp. 760–766, 2010.
[6] I. Coddington, N. Newbury, and W. Swann, "Dual-comb spectroscopy," *Optica*, vol. 3, no. 4, pp. 414, 2016.
[7] J. Ye, "Absolute measurement of a long, arbitrary distance to less than an optical fringe," *Opt. Lett.*, vol. 29, no. 10, pp. 1153–1155, 2004.
[8] K. Minoshima and H. Matsumoto, "High-accuracy measurement of 240-m distance in an optical tunnel by use of a compact femtosecond laser," *Appl. Opt.*, vol. 39, no. 30, pp. 5512–5517, 2000.
[9] K. N. Joo and S. W. Kim, "Absolute distance measurement by dispersive interferometry using a femtosecond pulse laser," *Opt. Exp.*, vol. 14, no. 13, pp. 5954–5969, 2006.
[10] N. Schuhler, Y. Salvad, S. Lvque, R. Dndliker, and R. Holzwarth, "Frequency-comb-referenced two-wavelength source for absolute distance measurement," *Opt. Lett.*, vol. 31, no. 21, pp. 3101–3103, 2006.

[11] J. Jin, Y. J. Kim, Y. Kim, and S. W. Kim, "Absolute distance measurements using the optical comb of a femtosecond pulse laser," *Int. J. Precision Eng. Manuf.*, vol. 8, no. 4, pp. 22–26, 2007.
[12] K. N. Joo, Y. Kim, and S. W. Kim, "Distance measurements by combined method based on a femtosecond pulse laser," *Opt. Exp.*, vol. 16, no. 24, pp. 19799–19806, 2008.
[13] L. Lee, Y. J. Kim, K. Lee, S. Lee, and S. W. Kim, "Time-of-flight measurement with femtosecond light pulses," *Nat. Photon.*, vol. 4, no. 10, pp. 716–720, 2010.
[14] I. Coddington, W. C. Swann, L. Nenadovic, and N. R. Newbury, "Rapid and precise absolute distance measurements at long range," *Nat. Photon.*, vol. 3, no. 6, pp. 351–356, 2009.
[15] X. Zhao *et al.*, "Picometer-resolution dual-comb spectroscopy with a free-running fiber laser," *Opt. Exp.*, vol. 24, no. 19, pp. 21833–21845, 2016.
[16] T. Ideguchi, T. Nakamura, Y. Kobayashi, and K. Goda, "Kerr-lens mode-locked bidirectional dual-comb ring laser for broadband dual-comb spectroscopy," *Optica*, vol. 3, no. 7, pp. 748–753, 2016.
[17] T. A. Liu, N. R. Newbury, and I. Coddington, "Sub-micron absolute distance measurements in sub-millisecond times with dual free-running femtosecond Er fiber-lasers," *Opt. Exp.*, vol. 19, no. 19, pp. 18501–18509, 2011.
[18] T. W. Liu, C. M. Wu, Y. C. Hsu, and W. Y. Chen, "Dual Ti:Sapphire comb lasers by a fiber laser pumping scheme and a hand-sized optical frequency reference," *Appl. Phys. B*, vol. 117, no. 2, pp. 699–705, 2014.
[19] R. Yang, F. Pollinger, K. Meiners-Hagen, J. Tan, and H. Bosse, "Heterodyne multi-wavelength absolute interferometry based on a cavity-enhanced electro-optic frequency comb pair," *Opt. Lett.*, vol. 39, no. 20, pp. 5834–5837, 2014.
[20] D. A. Long *et al.*, "Multiheterodyne spectroscopy with optical frequency combs generated from a continuous-wave laser," *Opt. Lett.*, vol. 39, no. 9, pp. 2688–2690, 2014.
[21] X. Zhao *et al.*, "Switchable, dual-wavelength passively mode-locked ultrafast fiber laser based on a single-wall carbon nanotube modelocker and intracavity loss tuning," *Opt. Exp.*, vol. 19, no. 2, pp. 1168–1173, 2011.
[22] P. E. Ciddor and R. J. Hill, "Refractive index of air. 2. Group index," *Appl. Opt.*, vol. 38, no. 9, pp. 1663–1667, 1999.
[23] G. Wu, S. Xiong, K. Ni, Z. Zhu, and Q. Zhou, "Parameter optimization of a dual-comb ranging system by using a numerical simulation method," *Opt. Exp.*, vol. 23, no. 25, pp. 32044–32053, 2015.